

Self-Consistent Calculations of Block Copolymer Solution Phase Behavior

Ching-I Huang* and Timothy P. Lodge*

Department of Chemistry and Department of Chemical Engineering & Materials Science, University of Minnesota, Minneapolis, Minnesota 55455-0431

Received January 5, 1998; Revised Manuscript Received April 13, 1998

ABSTRACT: We present a theoretical study of the influence of solvent on ordered block copolymer solutions. The phase behavior is examined as a function of solvent selectivity, temperature, copolymer concentration, composition, and molecular weight. Phase maps are constructed using self-consistent mean-field (SCMF) theory, via the relative stability of the “classical” phases, lamellae (L), hexagonally packed cylinders (C), and a body-centered cubic array of spheres (S). Solvent selectivity and polymer concentration strongly influence phase transitions in copolymer solutions. When a neutral good solvent is added to a symmetric block copolymer, a direct (lyotropic) transition from L to disordered (D) is expected, analogous to the (thermotropic) L → D transition in melts. Indeed for neutral good solvents the dilution approximation is followed: the phase map is equivalent to that in the melt, once the interaction parameter is multiplied by the copolymer volume fraction. In contrast, for a symmetric block copolymer in the presence of a slightly selective solvent, the progression L → C → S → micelles → D is expected, although the micellar phase is not treated here. For asymmetric copolymers more elaborate sequences are anticipated, such as the progression C_B → L → C_A → S_A → micelles → D. The stability limit of a homogeneous block copolymer solution is also examined via the random phase approximation (RPA) method. The effect of polymer concentration on the spinodal instability falls into two regimes. When the solvent is not very selective, the stable microphase separation region is reduced as polymer concentration decreases, whereas for very selective solvents, whereas for very selective solvents decreasing polymer concentration broadens the region of stable ordered microstructures.

Introduction

Block copolymers have attracted considerable attention due to their ability to self-assemble into various ordered structures. Much of the research to date has emphasized bulk block copolymers.^{1–4} Consequently, the factors governing the self-assembly of AB block copolymer melts are well understood, although some interesting questions remain. In general, the immiscibility of the A and B blocks (quantified by the interaction parameter χ) drives the system to segregate as temperature decreases ($\chi \sim T^{-1}$). Due to the connectivity of the blocks, the system undergoes an order–disorder transition into A-rich and B-rich microdomains at a certain value of χN , where N is the degree of polymerization. The composition of the copolymer, $f = (N_A / [N_A + N_B])$, largely determines the shape and packing symmetry of the ordered microstructures. The so-called “classical” phases, such as lamellae, hexagonal cylinders, and body-centered cubic spheres, and more complicated phases, such as the gyroid, double diamond, and perforated layered phases, have been examined both theoretically and experimentally. However, it is often difficult to achieve the order–disorder transition temperature with useful (i.e., high) molecular weight samples. Microphase-separated samples can be prepared from solution, where the unfavorable monomer–monomer interactions are partly screened. The addition of a second, lower molecular weight component may also impart desirable properties, e.g., as tackifiers in pressure-sensitive adhesives. With the addition of a diluent, the phase behavior becomes more complicated due to the extra degrees of freedom. In addition to order–

order and order–disorder transitions, macrophase separation and regions of two-phase coexistence are expected.

Previous theoretical studies of block copolymer solution phase behavior have addressed some of these issues.^{5–15} For example, Hong and Noolandi considered neutral solvents and demonstrated the possibility of macrophase separation into solvent-rich and copolymer-rich phases when the solvent is poor.^{5,6} However, they did not consider order–order transitions within the ordered phase or the inhomogeneous distribution of solvent. Whitmore and Noolandi employed a self-consistent mean-field (SCMF) scheme to examine lamellar copolymers in neutral good solvents and quantified the solvent inhomogeneity as well as the concentration dependence of the lamellar spacing.¹⁰ Whitmore and Vavasour extended these calculations to the cylindrical and spherical microphases.¹⁴ In the concentrated regime and when the solvent is neutral and good, the solution phase behavior follows the “dilution approximation”:¹⁶ for any composition f , the mean-field order–disorder transition (ODT) and order–order transitions (OOT) can be obtained from the melt phase map by replacing $\chi_{AB}N$ with $\phi\chi_{AB}N$, where ϕ is the copolymer volume fraction. Thus, $(\phi\chi_{AB}N)_{\text{ODT},\text{OOT}} = F(f)$, where χ_{AB} is the A–B interaction parameter. In semidilute solutions chain swelling effects cannot be ignored, and Olvera de la Cruz⁸ and Fredrickson and Leibler⁷ have predicted a different result for the ODT: $(\phi^{1.59}\chi_{AB}N)_{\text{ODT}} = F(f)$. Birshtein and Zhulina considered the effects of swelling for strongly segregated copolymers.¹⁵ Banaszak and Whitmore initiated the investigation of slightly selective solvents with the lamellar phase, and examined the domain spacing as a function of ϕ , χ , and N .¹³

* To whom correspondence should be addressed.

Experimental studies of concentrated copolymer solution phase behavior in nominally neutral solvents have largely focused on poly(styrene-*b*-isoprene) copolymers in toluene and dioctyl phthalate.^{17–20} The results are in good agreement with SCMF theory in some respects, e.g., the concentration dependence of the lamellar period, but not in others; for example, the ODT concentration for symmetric diblock copolymers does not follow the “dilution approximation”,¹⁹ even though the addition of solvent stabilizes the disordered phase. Selective solvents have been more extensively studied, such as poly(ethylene oxide-*b*-propylene oxide-*b*-ethylene oxide) in water²¹ and styrene–diene copolymers in, e.g., hexadecane and dibutyl phthalate.^{22–25} Recently, we demonstrated a simple SANS method to quantify the distribution of neutral and selective solvents in ordered block copolymer solutions.²⁶ This study revealed that, inter alia, even a very slight degree of selectivity could lead to a measurable preferential swelling of one component and that this selectivity could be quantified.

In addition to solvent selectivity, the effects of other parameters, such as concentration, temperature, copolymer composition, and molecular weight, also need to be considered. In this paper we employ SCMF theory to examine the phase behavior of block copolymers in the presence of a solvent. These results extend the previous work of Whitmore and co-workers,^{10,13,14} although the numerical scheme is actually based on that applied to melts by Matsen.²⁷ For simplicity, we restrict consideration to the classical phases in order to construct the phase maps; the effect of solvent on the nonclassical phases will be deferred to a future report. We also locate the spinodal instability of the disordered phase by using the random phase approximation (RPA), from which the effect of solvent on both microphase and macrophase transitions is revealed.

Theory

We use self-consistent mean-field (SCMF) theory to examine block copolymer solution phase behavior. Although this mean-field approach ignores the potentially important contributions of both chain swelling^{7,8} and thermal fluctuations,^{28–30} we anticipate that the SCMF theory should enjoy similar success in predicting the qualitative phase behavior in concentrated block copolymer solutions as it does in melts, at least for high concentrations. The applicability of the SCMF theory to copolymer systems has recently been reviewed.^{31,32} We extend the recent SCMF scheme of Matsen, which was developed to study phase behavior in melts.²⁷ The method introduces a series of orthonormal basis functions, $f_j(r)$, to express any given function, $g(r)$, in terms of the corresponding amplitudes, g_j , i.e., $g(r) = \sum_j g_j f_j(r)$. The basis functions reflect the symmetry of the ordered phase being considered, and are chosen to be eigenfunctions of the Laplacian operator

$$\nabla^2 f_j(r) = -\lambda_j L^{-2} f_j(r) \quad (1)$$

where L is the length scale for the ordered phase. The basis functions are ordered starting with $f_0(r) = 1$ such that λ_j is an increasing series. For lamellae $f_j(r) = 2^{1/2} \cos(2\pi j x/L)$, $j \geq 1$, where x is the coordinate orthogonal to the lamellae. Basis functions for the phases with other space-group symmetries can be found in ref 33.

We consider a solution of AB diblock copolymer and solvent, present at average volume fractions ϕ and $1 -$

ϕ , respectively, and assume the system is incompressible, both locally and globally. Each polymer chain has degree of polymerization N , and A-monomer fraction f . It is assumed that each monomer type has the same statistical segment length b . The local interaction between each pair of units α and β is quantified by the Flory interaction parameter $\chi_{\alpha\beta}$. Each polymer is parametrized with a variable s that increases from 0 to 1 along its length. We assume that the A-block starts from $s = 0$ and terminates at $s = f$, which is the A–B junction point. Using this parametrization, it is convenient to define two end-segment copolymer distribution functions, $q_C(r,s)$ and $q_C^+(r,s)$ which are found by integrating all possible configurations subject to the fields $\omega_A(r)$ and $\omega_B(r)$ for chain segments running from $s = 0$ to f and from $s = f$ to 1, respectively. The distribution function $q_C(r,s)$ satisfies the modified diffusion equation

$$\frac{\partial q_C}{\partial s} = \begin{cases} \frac{1}{6} N b^2 \nabla^2 q_C - \omega_A q_C & \text{if } s < f \\ \frac{1}{6} N b^2 \nabla^2 q_C - \omega_B q_C & \text{if } s > f \end{cases} \quad (2)$$

and the initial condition, $q_C(r,0) = 1$. The equation for $q_C^+(r,s)$ is similar except that the right-hand side of eq 2 is multiplied by -1 , and the initial condition is $q_C^+(r,1) = 1$. Since there is no chain connectivity in the solvent case, the equation governing the solvent distribution function $q_S(r,s)$ becomes

$$\frac{\partial q_S}{\partial s} = -\omega_S(r) q_S \quad (3)$$

When the amplitudes corresponding to the basis functions are utilized, the amplitudes of the fields have to satisfy

$$\begin{aligned} \omega_{A,i} - \omega_{S,i} &= \chi_{AB} N \varphi_{B,i} + \chi_{AS} N \varphi_{S,i} - \chi_{AS} N \varphi_{A,i} - \chi_{BS} N \varphi_{B,i} \\ \omega_{B,i} - \omega_{S,i} &= \chi_{AB} N \varphi_{A,i} + \chi_{BS} N \varphi_{S,i} - \chi_{AS} N \varphi_{A,i} - \chi_{BS} N \varphi_{B,i} \\ \varphi_{A,i} + \varphi_{B,i} + \varphi_{S,i} &= \delta_{i0} \quad i = 0, 1, 2, \dots \end{aligned} \quad (4)$$

In turn, the amplitudes of the concentrations of A, B, and S are expressed in terms of the distribution functions

$$\begin{aligned} \varphi_{A,i} &= \frac{\phi}{q_{C,1}(1)} \sum_{j,k} \Gamma_{ijk} \int_0^f ds q_{C,j}(s) q_{C,k}^+(s) \\ \varphi_{B,i} &= \frac{\phi}{q_{C,1}(1)} \sum_{j,k} \Gamma_{ijk} \int_f^1 ds q_{C,j}(s) q_{C,k}^+(s) \\ \varphi_{S,i} &= q_{S,i} \left(\frac{1}{N} \right) \end{aligned} \quad (5)$$

where

$$\Gamma_{ijk} = \frac{1}{V} \int dr f_i(r) f_j(r) f_k(r) \quad (6)$$

and the modified diffusion eqs 2 and 3 in terms of $q_{C,i}(s)$, $q_{C,i}^+(s)$, and $q_{S,i}(s)$, become

$$\frac{\partial q_{C,i}}{\partial s} = \begin{cases} \sum_j A_{ij} q_{C,j} & \text{if } s < f \\ \sum_j B_{ij} q_{C,j} & \text{if } s > f \end{cases} \quad (7)$$

The equation for $q_{C,i}^+$ is similar except that the right-hand side is multiplied by -1 , and

$$\frac{\partial q_{S,i}}{\partial s} = \sum_j C_{ij} q_{S,j} \quad (8)$$

with the initial conditions, $q_{C,i}(s=0) = \delta_{i0}$, $q_{C,i}^+(s=1) = \delta_{i0}$, and $q_{S,i}(s=0) = \delta_{i0}$. The matrices A_{ij} , B_{ij} , and C_{ij} , are given by

$$\begin{aligned} A_{ij} &= -\frac{Nb^2}{6L^2} \lambda_i \delta_{ij} - \sum_k \omega_{A,k} \Gamma_{ijk} \\ B_{ij} &= -\frac{Nb^2}{6L^2} \lambda_i \delta_{ij} - \sum_k \omega_{B,k} \Gamma_{ijk} \\ C_{ij} &= -\sum_k \omega_{S,k} \Gamma_{ijk} \end{aligned} \quad (9)$$

Once the above amplitudes are determined and the self-consistent equations for the fields are satisfied, the free energy per molecule F is given by

$$\begin{aligned} \frac{F}{k_B T} &= -\phi \ln \left[\frac{q_{C,1}(1)}{\phi} \right] - (1-\phi) N \ln \left[\frac{q_{S,1}(1/N)}{1-\phi} \right] - \\ &\sum_i (\omega_{A,i} \varphi_{A,i} + \omega_{B,i} \varphi_{B,i} + \omega_{S,i} \varphi_{S,i}) + \sum_i (\chi_{AB} N \varphi_{A,i} \varphi_{B,i} + \\ &\chi_{AS} N \varphi_{A,i} \varphi_{S,i} + \chi_{BS} N \varphi_{B,i} \varphi_{S,i}) \end{aligned} \quad (10)$$

which reduces to the Flory–Huggins mean-field free energy functional in the disordered state. For a periodic ordered phase, we minimize the free energy with respect to the lattice spacing L ; to determine the most stable phase one compares free energies of different possible phases.

The stability limit of a disordered phase, i.e., the spinodal, is determined by applying the random phase approximation (RPA) to diblock copolymer solutions; the details have been provided.⁷ In block copolymer solutions, it is convenient to expand free energies in terms of two-order parameters $\Psi_1(r)$ and $\Psi_2(r)$, given by

$$\begin{aligned} \Psi_1(r) &= \frac{1-f}{\phi} \delta\phi_A(r) - \frac{f}{\phi} \delta\phi_B(r) \\ \Psi_2(r) &= \delta\phi_A(r) + \delta\phi_B(r) \end{aligned} \quad (11)$$

where $\delta\phi_\alpha(r)$ is the fluctuation in concentration about the mean value of component α . The order parameter $\Psi_1(r)$ is a nonzero periodic function if the solution is microphase separated, and the parameter $\Psi_2(r)$ describes the nonuniformity in solvent concentration.

In terms of these two order parameters, the resulting Landau expression for the free energy of a diblock copolymer in a solvent is

$$\frac{F}{Nk_B T} = \frac{F_0}{Nk_B T} + \frac{1}{2!} V^{-2} \sum_{k,\alpha,\beta} R_{\alpha\beta}(k) \psi_\alpha(k) \psi_\beta(k) + \text{higher order terms} \quad (12)$$

where $\psi_\alpha(k)$ is the Fourier transform of the $\Psi_\alpha(r)$, and F_0 is the Flory–Huggins mean-field free energy functional per molecule. The coefficients R_{IJ} , $I, J = 1, 2$, are related to the correlation functions of noninteracting Gaussian diblock chains $S_{\alpha\beta}(k)$, where $\alpha, \beta = A, B$, and are given by

$$R_{11}(k) = \phi \left[\frac{\Sigma(k)}{W(k)} - 2\chi_{AB}\phi \right]$$

$$\begin{aligned} R_{12}(k) &= R_{21}(k) = \\ &\frac{f(S_{BB}(k) + S_{AB}(k)) - (1-f)(S_{AA}(k) + S_{AB}(k))}{W(k)} + \\ &\frac{1-f}{1-\phi} + 2f(1-f)\chi_{AB} - 2f\chi_{AS} - 2(1-f)\chi_{BS} \end{aligned} \quad (13)$$

$$\begin{aligned} R_{22}(k) &= \\ &\frac{(1-f)^2 S_{AA}(k) + f^2 S_{BB}(k) - 2f(1-f)S_{AB}(k)}{\phi W(k)} + \\ &\frac{1}{1-\phi} + 2f(1-f)\chi_{AB} - 2f\chi_{AS} - 2(1-f)\chi_{BS} \end{aligned} \quad (13)$$

with

$$\Sigma(k) = S_{AA}(k) + 2S_{AB}(k) + S_{BB}(k)$$

$$W(k) = S_{AA}(k)S_{BB}(k) - S_{AB}^2(k)$$

$$S_{AA}(k) = Ng(f, x)$$

$$S_{AB}(k) = \frac{1}{2} N [g(1, x) - g(f, x) - g(1-f, x)]$$

$$S_{BB}(k) = Ng(1-f, x) \quad (14)$$

where $x = k^2 R_g^2$ (R_g is the radius of gyration), and $g(f, x)$ is the modified Debye function, given by

$$g(f, x) = \frac{2}{x^2} (fx + \exp(-fx) - 1) \quad (15)$$

Hence, the spinodal line of a disordered state is obtained by solving

$$\begin{aligned} \det R &= \begin{vmatrix} R_{11}(k) & R_{12}(k) \\ R_{21}(k) & R_{22}(k) \end{vmatrix}_{k^*} = 0 \\ \frac{\partial}{\partial k} (\det R)|_{k^*} &= 0 \end{aligned} \quad (16)$$

Results and Discussion

In contrast to copolymer melts, for which a universal phase map³⁴ can be constructed in terms of $\chi_{AB}N$ and f , the phase maps of copolymer solutions depend on f , N , ϕ , χ_{AB} , χ_{AS} , and χ_{BS} . The selectivity of the solvent is determined by the relative values of χ_{AS} and χ_{BS} . For example, the solvent is neutral when $\chi_{AS} = \chi_{BS}$, whereas the solvent is selective for B when $\chi_{AS} > \chi_{BS}$. A schematic “phase cube” can be constructed in terms of f , ϕ , and $\chi_{AB}N$ for block copolymers with a particular value of N in the presence of a solvent with the

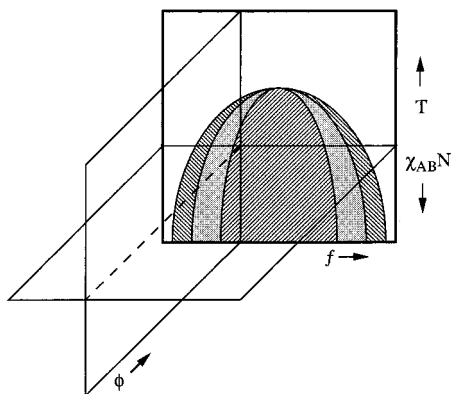
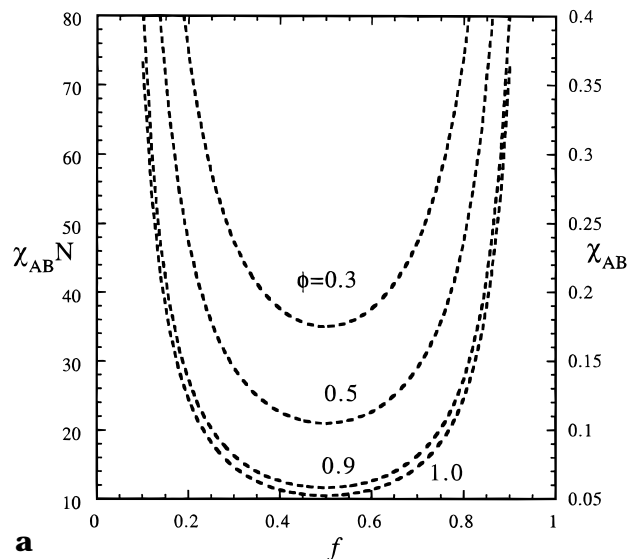


Figure 1. Phase cube for diblock copolymer solutions in terms of polymer concentration ϕ , copolymer composition f , and degree of copolymer segregation $\chi_{AB}N$, for a polymer with degree of polymerization N in the presence of a solvent with interaction parameters χ_{AS} and χ_{BS} . The horizontal plane denotes a constant temperature slice (ϕ vs f), and the vertical planes denote a phase diagram for a particular copolymer (ϕ vs T) or a phase map for a given concentration (T vs f).

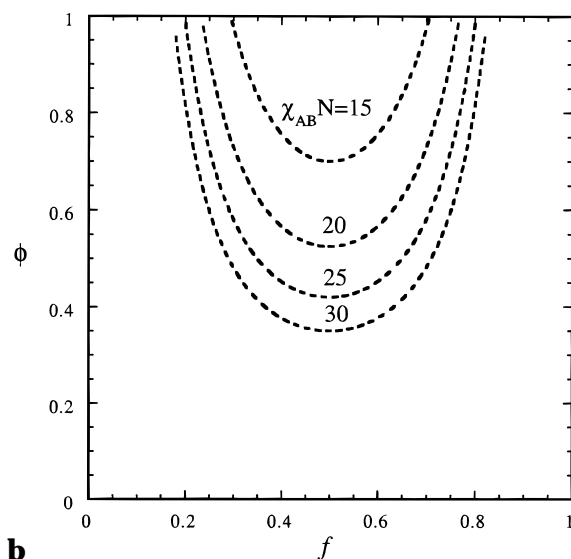
interaction parameters χ_{AS} and χ_{BS} (see Figure 1). The four vertical faces of the prism correspond to: the copolymer melt as a function of f (rear face), solutions of A and B homopolymers in S (side faces), and the pure solvent S (front face); the vertical axis is temperature. Three orthogonal planes across the cube are indicated: constant copolymer concentration ϕ , constant copolymer composition f (i.e., a particular copolymer molecule) and constant temperature (or χN). However, one cube is insufficient to incorporate all the possibilities, because the three χ parameters will have different dependences on T and because N and χ_{AB} can have separable effects.

We first examine how solvent selectivity affects the stability of a disordered block copolymer solution, by constructing the spinodal curves in the phase cube for different values of χ_{AS} at constant χ_{BS} . We then study the effect of the solvent selectivity on the resulting ordered block copolymer microstructures. As noted above, equilibrium phase maps are developed based on the stability of the classical phases only: spheres of A (S_A), cylinders of A (C_A), lamellae (L), cylinders of B (C_B), and spheres of B (S_B).

Spinodal of a Homogeneous Solution. In Figures 2–4, N is fixed at 200 and $\chi_{BS} = 0.4$, and the stability limits are examined in terms of ϕ , f , and $\chi_{AB}N$, for χ_{AS} equal to 0.4, 0.6, and 0.8, respectively. We present two-dimensional spinodal curves at constant ϕ and constant $\chi_{AB}N$ in parts a and b of each figure, respectively. Figure 2 thus corresponds to a neutral good solvent, as $\chi = 0.4$ is a typical value for a polymer in a good solvent. As expected, for any composition of a block copolymer in the neutral solvent, the stability limit of a homogeneous copolymer solution can be obtained directly from the melt curve, $(\chi_{AB}N\phi)_s = F(f)$. This prediction, the dilution approximation discussed in the Introduction, is illustrated in Figure 2a. Because the value of k^* obtained from eq 16 is greater than 0, the spinodal instability corresponds to an ordered phase. As ϕ decreases, $(\chi_{AB}N)_s$ increases: decreasing ϕ thus expands the disordered phase. For $\chi_{AB}N < 10.495$, any block copolymer in a neutral good solvent will form a homogeneous solution. For a constant $\chi_{AB}N > 10.495$, there exists a spinodal curve as shown in Figure 2b, within which a block copolymer system exhibits a stable ordered structure. As $\chi_{AB}N$ increases, this ordered



a

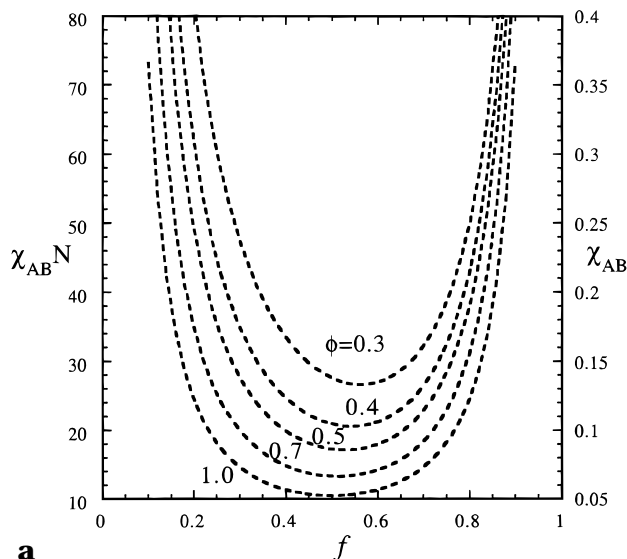


b

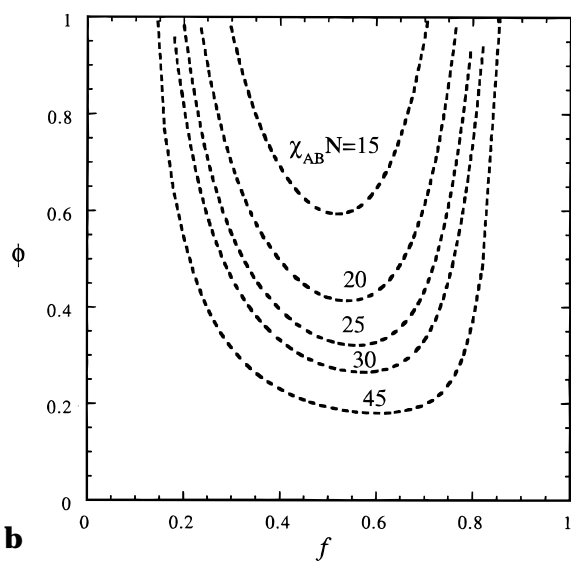
Figure 2. Two-dimensional spinodal curves for a disordered block copolymer solution with $N = 200$, $\chi_{AS} = 0.4$, and $\chi_{BS} = 0.4$, for constant ϕ (a), and $\chi_{AB}N$ (b).

region broadens. It should be noted that the dilution approximation is expected to fail when ϕ is small, as chain swelling becomes important. It should also break down when the solvent is neutral but poor, as the resulting spinodal curves may correspond to a macrophase separation between solvent-rich and copolymer-rich phases when $\phi\chi_{AB}N$ is large.

When χ_{AS} increases from 0.4 to 0.6, the region of stable ordered microdomains is enlarged, as shown in parts a and b of Figure 3. The solvent is thus of lower quality than a Θ solvent for the A block. Nevertheless, due to the high polymer volume fractions phase separation is not predicted (recall that the critical concentration for a homopolymer solution occurs at very low concentration). Although the stability limits do not follow the dilution approximation in terms of ϕ , f , and $\chi_{AB}N$ when the solvent is slightly selective, the trends are similar to those in the neutral solvent (Figure 2), with the spinodals skewing to $f > 0.5$. However, when the solvent becomes more strongly selective, e.g., when χ_{AS} increases to 0.8, the two-dimensional spinodal curves at constant ϕ and $\chi_{AB}N$ in parts a and b of Figure 4,



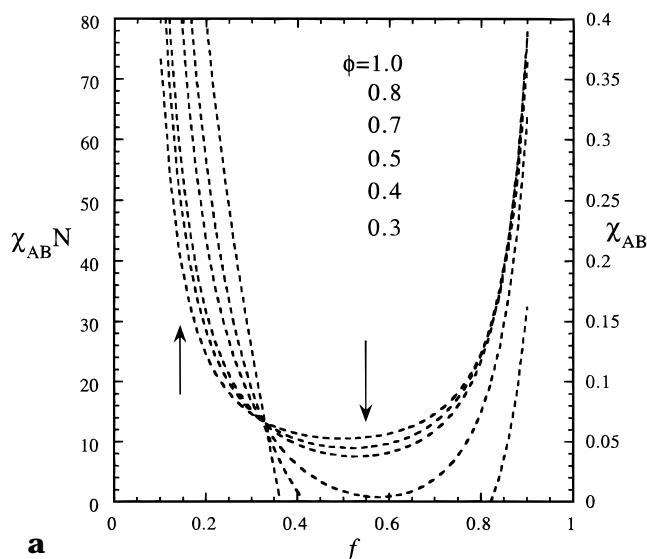
a



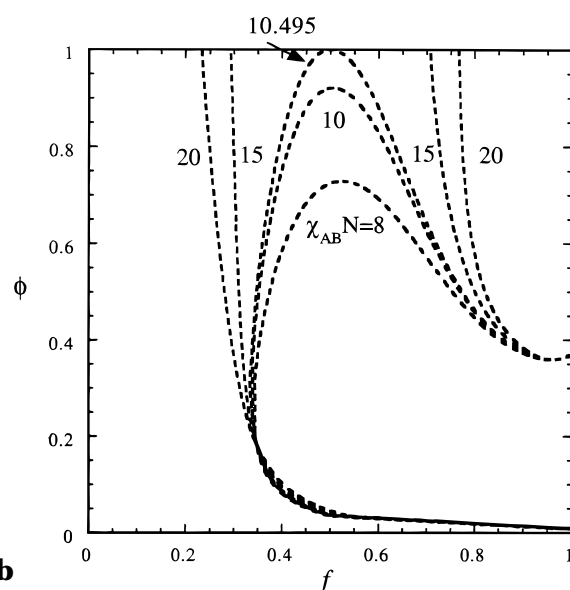
b

Figure 3. Two-dimensional spinodal curves for a disordered block copolymer solution with $N = 200$, $\chi_{AS} = 0.6$, and $\chi_{BS} = 0.4$, for constant ϕ (a) and $\chi_{AB}N$ (b).

respectively, become quite different from the results in Figures 2 and 3. In Figure 4a, the effect of polymer concentration ϕ on the spinodal exhibits two regimes. When f is small (< 0.33 in this case), $(\chi_{AB}N)_s$ increases with decreasing ϕ , as in Figures 2a and 3a. In contrast, for $f > 0.33$, $(\chi_{AB}N)_s$ decreases as ϕ decreases. In this region, the addition of a strongly B-selective solvent can induce either macro- or microphase separation, even when $\chi_{AB}N < 10.495$. As shown in Figure 4b, corresponding spinodal curves are observed for constant $\chi_{AB}N < 10.495$. The intersection of these curves with the vertical axis ($f = 1.0$) indicates that there exists a region of the homopolymer A solution which is unstable to macrophase separation between the A-rich and the solvent-rich disordered phases, as expected with a poor solvent for A. As $\chi_{AB}N$ increases, the area bounded by the spinodal curve continues to expand and touches the horizontal axis ($\phi = 1$) for a symmetric block copolymer melt when $\chi_{AB}N = 10.495$. When $\chi_{AB}N$ continues to increase, the spinodal curve splits into two. For any system between these two lines, when ϕ is close to 1.0, the system is unstable to the formation of an ordered



a



b

Figure 4. Two-dimensional spinodal curves for a disordered block copolymer solution with $N = 200$, $\chi_{AS} = 0.8$, and $\chi_{BS} = 0.4$, for constant ϕ (a) and $\chi_{AB}N$ (b). The arrows in part a indicate the order of curves for decreasing ϕ .

microstructure. As ϕ continues to decrease and/or when f is close to 1.0, the wave vector associated with the instability, k^* , approaches zero and the system can undergo a macrophase separation into the solvent-rich and the copolymer-rich disordered phases. It can also separate into solvent-rich disordered and copolymer-rich ordered phases.

As noted above, the effect of solvent selectivity on the stability limit of a homogeneous solution falls into two regimes. For a given diblock copolymer (f/N), there exists a crossover value χ_{AS}^* determined from the intersection of the two-dimensional spinodal curves as a function of $\chi_{AB}N$, ϕ , and χ_{AS} . For example, in Figure 5 the spinodal curves for $f = 0.5$ and $N = 200$ are shown, and the value of χ_{AS}^* is around 0.7. When the solvent is only slightly selective, $\chi_{AS} < \chi_{AS}^*$, decreasing ϕ will stabilize the homogeneous solution. In contrast, when the solvent is more strongly selective, $\chi_{AS} > \chi_{AS}^*$, the regions of stable ordered microstructures and/or macrophase separation are enlarged as ϕ decreases. The

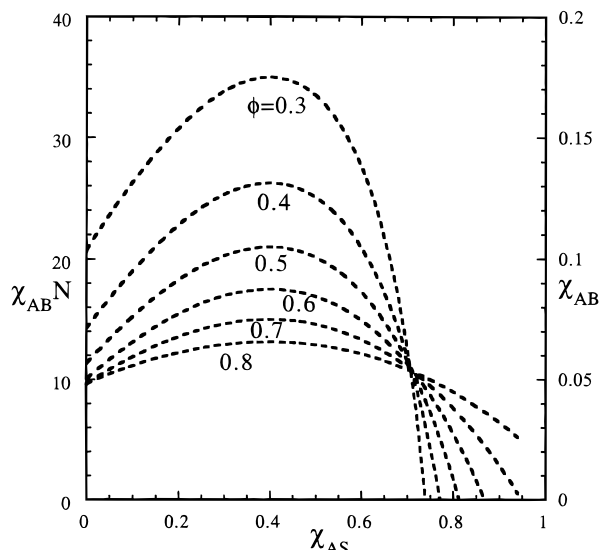
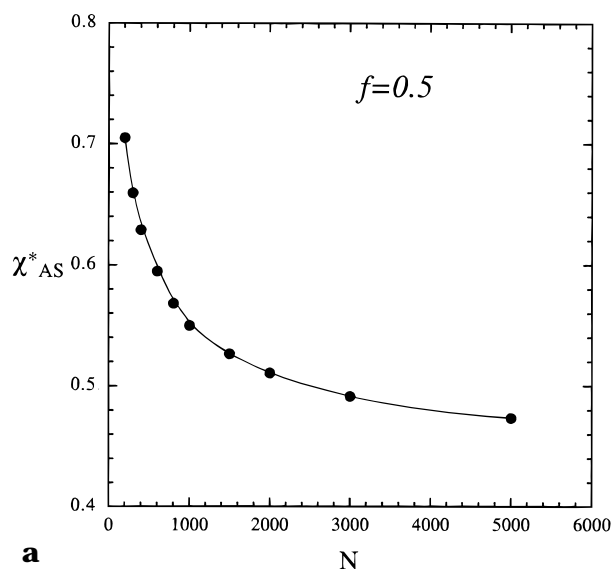


Figure 5. Two-dimensional spinodal curves for a disordered block copolymer solution as a function of ϕ , χ_{AS} , and $\chi_{AB}N$ for $f = 0.5$, $N = 200$, and $\chi_{BS} = 0.4$.

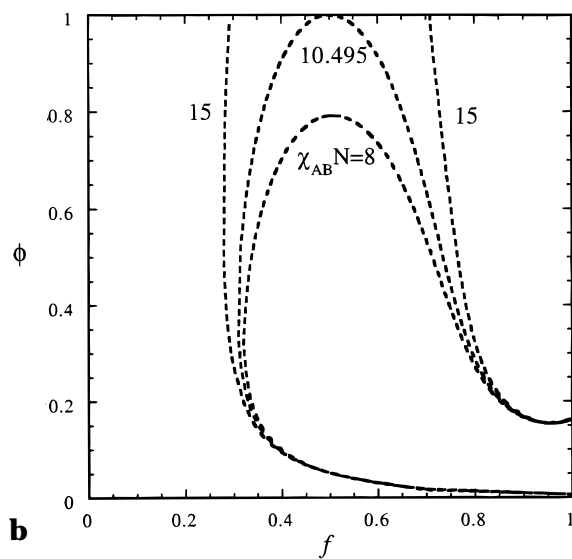
value of χ_{AS}^* depends on N : as N increases, χ_{AS}^* becomes smaller, as shown in Figure 6a for $f = 0.5$. This is understandable, as the solubility of A homopolymers decreases with increasing N for a given χ_{AS} . This N dependence is underscored in Figure 6b, where the two-dimensional spinodal curves are plotted for the same interaction parameters as in Figure 3, but with N increased from 200 to 1000; the character of the curves changes significantly.

Phase Maps of Block Copolymer Solutions: Neutral Solvents. To study the effect of the solvent in the ordered state, we constructed the phase maps for $N = 200$, as macrophase separation is not predicted for the segregation regime studied here. However, macrophase separation may be anticipated under certain circumstances for larger N . Although the value of N will affect the solution phase maps both quantitatively and qualitatively, the trends in phase behavior for fixed $N = 200$ are general.

In Figure 7a, we constructed the phase behavior of block copolymers in the presence of a neutral solvent for two different copolymer concentrations ϕ . We replot these data in Figure 7b rescaled as $\chi_{AB}\phi$ values to examine if the "dilution approximation" holds for both order-order and order-disorder transitions. We also compare our rescaled results with the melt phase map of Matsen,²⁷ which includes the gyroid (G) phase. It is clear that the boundaries between D/S and S/C and the spinodal of the disordered phase (D) follow the dilution approximation in the segregation regime studied here. These results agree with those of Whitmore and Vavasour, who considered the classical phases over the concentration range $0.1 \leq \phi \leq 0.8$.¹⁴ Although the complex phases are ignored in our calculations, we suspect that the dilution approximation will still be a reasonable approximation for G and that the rescaled phase map should reduce to Matsen's melt phase map in the weak and/or intermediate segregated regions; calculations involving the G phase in solution are currently in progress. As noted above, the dilution approximation should fail when $\chi_{AB}\phi$ is large and when ϕ is small, as macrophase separation may occur and/or the excluded-volume interactions need to be considered.



a



b

Figure 6. (a) The crossover χ_{AS}^* as a function of degree of copolymerization N . (b) Two-dimensional spinodal curves for a system as in Figure 3b but with $N = 1000$.

Also, the as-yet not fully understood experimental failure of the dilution approximation in concentrated solutions¹⁹ should be recalled.

Hong and Noolandi predicted qualitative macrophase separation of this system into a solvent-rich disordered phase and a copolymer-rich disordered phase.^{5,6} They also predicted a separation into a solvent-rich disordered phase and a copolymer-rich ordered phase, where they assumed the ordered microstructure to be lamellar. Our calculations extend their results, and those of Whitmore and Vavasour,¹⁴ and the qualitative effects of solvent quality and solvent amount on the phase behavior of neutral block copolymer solutions ($\chi_{AS} = \chi_{BS}$) can be summarized as follows.

When the solvent is poor (i.e., $\chi_{AS} > 0.5$), for a system at a constant ϕ , as $\chi_{AB}N$ increases, a phase transition from a single, homogeneous disordered phase into a two-phase region of solvent-rich and copolymer-rich disordered phases is expected. This is not surprising since we are dealing with a poor solvent. As $\chi_{AB}N$ continues to increase, the disordered copolymer-rich phase tends to form an ordered microstructure (O), and a further

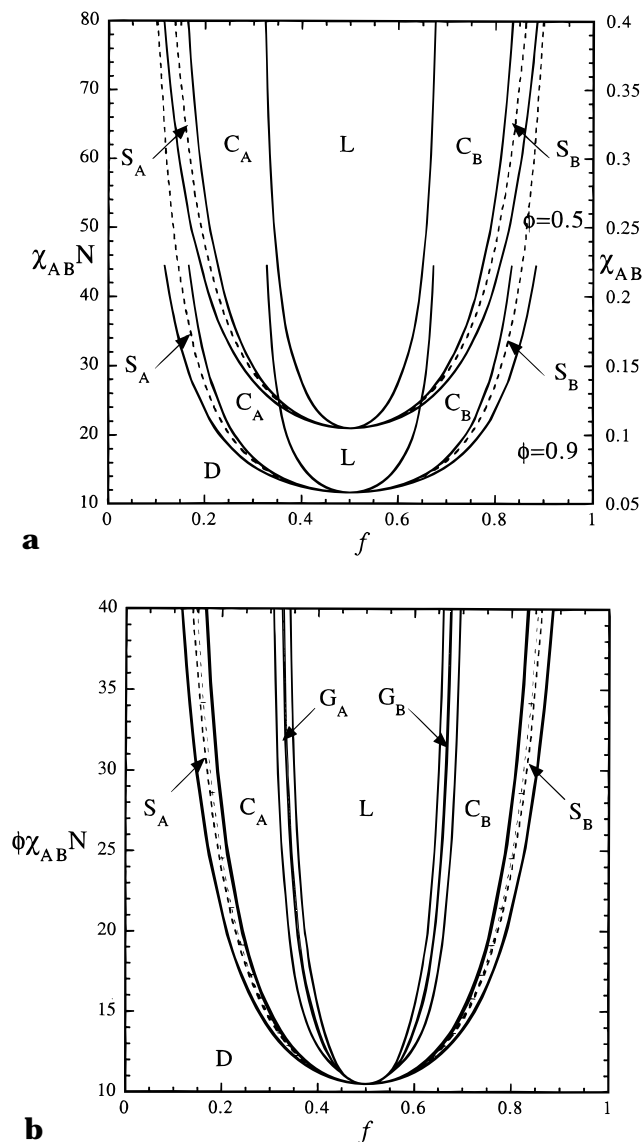


Figure 7. (a) Two-dimensional phase map for a diblock copolymer with $N = 200$ in a neutral good solvent ($\chi_{AS} = \chi_{BS} = 0.4$) for constant ϕ . (b) Rescaled phase maps from part a in compared with the melt. The melt calculation includes the G phase, whereas the solution ones do not. The dashed curves correspond to the spinodal instability of the disordered state.

phase transition from a two-phase D/D into a two-phase D/O is expected. It should be noted that inside the two-phase D/O region, a transition of ordered microdomains from $S \rightarrow C \rightarrow G \rightarrow L$ is possible (although we do not consider G explicitly). When $\chi_{AB}N$ is fixed at a value in the weak and intermediate segregation regime, as ϕ continues to decrease, a transition from O ($L \rightarrow G \rightarrow C \rightarrow S$) to D is expected according to the dilution approximation. Furthermore, due to the poor solvent quality, a macrophase separation from D \rightarrow two-phase D/D occurs when ϕ is very small. When $\chi_{AB}N$ is very large, there should be a sequence of O ($L \rightarrow G \rightarrow C \rightarrow S$) \rightarrow two-phase D/O as ϕ decreases.

On the other hand, when the solvent is good (i.e., $\chi_{AS} < 0.5$), no macrophase separation occurs. Therefore, at a constant ϕ , a sequence D \rightarrow O ($S \rightarrow C \rightarrow G \rightarrow L$) of transitions may be expected by increasing $\chi_{AB}N$. If $\chi_{AB}N$ is fixed in the weak and intermediate region, as ϕ decreases, only the transition from O ($L \rightarrow G \rightarrow C \rightarrow S$) \rightarrow D is observed.

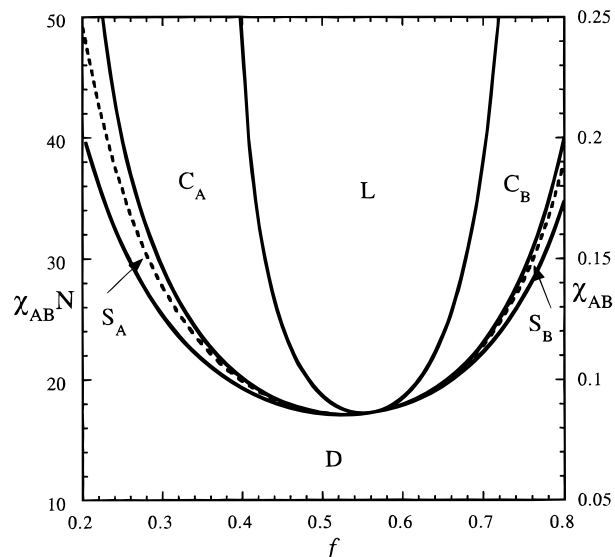


Figure 8. Two-dimensional phase map for a diblock copolymer with $N = 200$ in a selective solvent with $\chi_{AS} = 0.6$ and $\chi_{BS} = 0.4$ for $\phi = 0.5$.

Phase Maps of Block Copolymer Solutions: Selective Solvents. In reality, it is rare to find a perfectly neutral solvent, and thus it is of importance to examine how a small degree of solvent selectivity affects the phase behavior of block copolymer solutions. Furthermore, larger selectivities may be expected to produce larger qualitative changes in the phase behavior relative to the melt than in a neutral solvent. For a neutral solvent, increasing solvent concentration is analogous to increasing T , whereas addition of a selective solvent is similar to varying T and f simultaneously. In Figure 8, we show the phase map of a diblock copolymer in the presence of a selective solvent at $\phi = 0.5$. The interaction parameters χ_{AS} and χ_{BS} are set equal to 0.6 and 0.4, respectively. An interesting phenomenon is observed when $f = 0.5 - 0.56$. Although the A block is longer than the B block, the diblock still forms the "inverse" ordered bcc array of A-rich spheres, S_A , and inverse hexagonal A-rich cylinders, C_A , in the minority B matrix in the weak segregation regime. This is due to the fact that the solvent prefers the B block and thus acts in a manner that corresponds qualitatively to reducing f . To examine the solvent selectivity effect further, we set χ_{BS} equal to 0.4, and vary χ_{AS} . In Figure 9 we show the resulting phase map for symmetric block copolymers ($f = 0.5$) at $\phi = 0.5$ as a function of $\chi_{AB}N$ and χ_{AS} . As shown in Figure 9, even a very slightly selective solvent can induce first-order phase transitions from D $\rightarrow S_A \rightarrow C_A \rightarrow L$ as $\chi_{AB}N$ increases. In contrast, only the D \rightarrow L transition would be expected upon increasing $\chi_{AB}N$ in a perfectly neutral solution or melt. As the solvent becomes more selective, the ODT and OOT values of $\chi_{AB}N$ decrease: the solvent selectivity enlarges the regime of ordered microdomains. If $\chi_{AB}N$ is fixed at a certain value such that the copolymer in a neutral solvent would exhibit a single disordered phase, increasing χ_{AS} reveals a very narrow region of D $\rightarrow S_A \rightarrow C_A$ before the stable L phase is reached. This is due to the fact that when the solvent is not very selective, the copolymer composition still dominates the interfacial curvature. Since the blocks are symmetric, L is the most stable phase. However, when the solvent becomes very poor for A, the A blocks prefer to be near each other rather than the solvent. Therefore, L $\rightarrow C_A \rightarrow S_A$ is

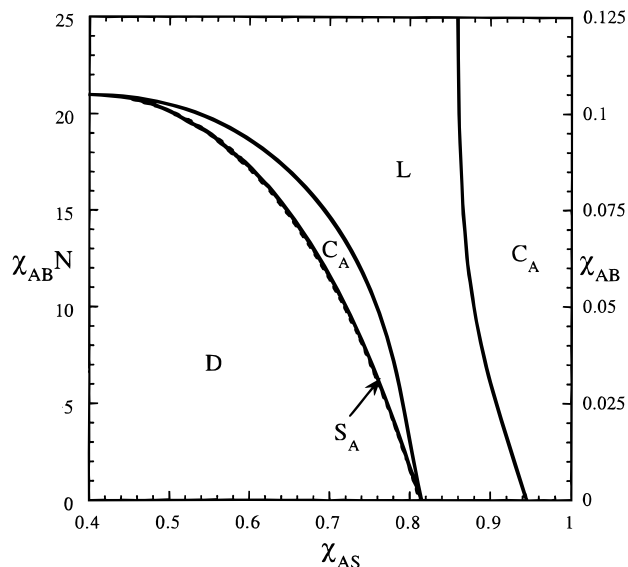


Figure 9. Two-dimensional phase map for a block copolymer solution with $f = 0.5$, $N = 200$, $\phi = 0.5$, and $\chi_{BS} = 0.4$ as a function of χ_{AS} and $\chi_{AB}N$.

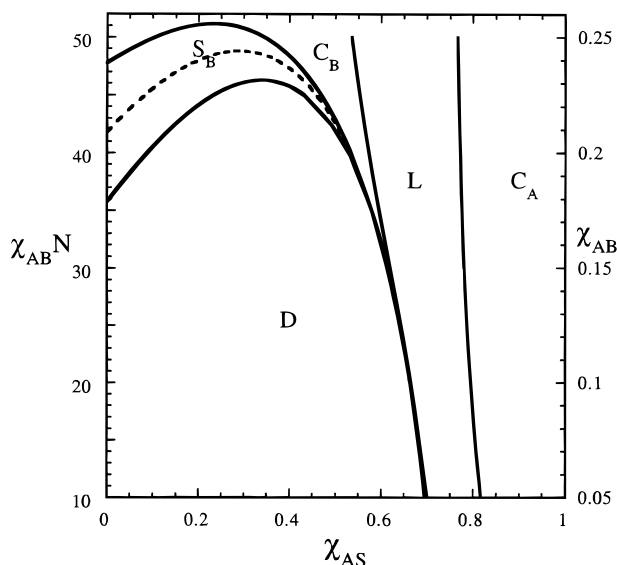


Figure 10. Two-dimensional phase map for a block copolymer solution with $f = 0.7$, $N = 200$, $\phi = 0.3$, and $\chi_{BS} = 0.4$ as a function of χ_{AS} and $\chi_{AB}N$.

expected upon further increasing χ_{AS} . Finally, this ordered block copolymer system demixes with a solvent-rich phase separating from an ordered microstructure. For the parameters in Figure 9, only a transition to the hexagonal phase is observed by the time χ_{AS} has increased to 1.0. However, when the degree of copolymerization N increases, and/or when more solvent is added, the system will undergo the above phase transitions at smaller χ_{AS} values. We point out that varying T for a given copolymer depicted in Figure 9 would correspond to a diagonal trace across the phase boundaries, as both axes depend on T .

The effect of solvent selectivity for asymmetric diblock copolymers is illustrated by the phase map for $f = 0.7$ and $\phi = 0.3$ shown in Figure 10. When a neutral solvent is added to copolymers with $f = 0.7$, only S_B and C_B would be stable in the ordered regime, as in the melt. With the addition of a good solvent selective for A ($\chi_{AS} < \chi_{BS}$), both phases remain stable in the ordered state,

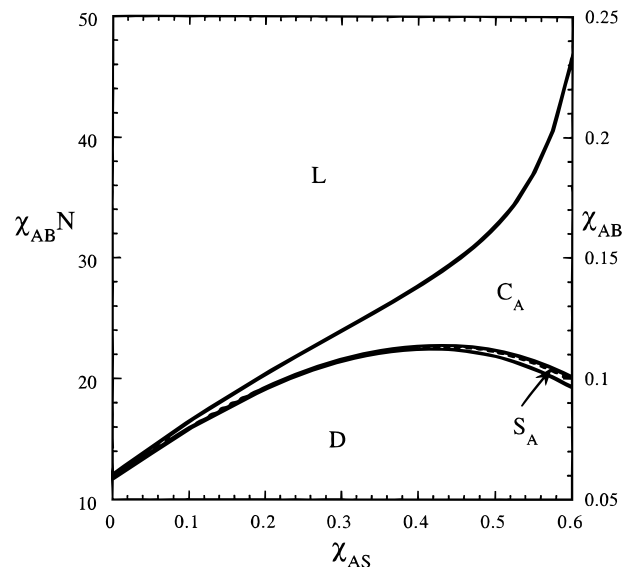


Figure 11. Two-dimensional phase map for a block copolymer solution with $f = 0.4$, $N = 200$, $\phi = 0.5$, and $\chi_{BS} = 0.4$ as a function of χ_{AS} and $\chi_{AB}N$.

with the S_B region enlarged. When a solvent selective for B is added, there exist additional phase transitions to the lamellar and the inverse hexagonal cylinders, C_A in this case, as χ_{AS} continues to increase. Further transitions to S_A and macrophase separation may be expected when the solvent is even more strongly selective for B. In general, similar behavior is expected for $f < 0.5$, but with A and B exchanged. For example, when $f < 0.5$ and $\chi_{AS} < \chi_{BS}$, inverse structures such as C_B and S_B may be observed. However, as is apparent from Figure 11, when $f = 0.4$ and $\phi = 0.5$, we observe no such stable phases when χ_{AS} decreases to 0. Rather, with $\chi_{AS} < \chi_{BS}$, L is found to be stable over most of this regime. This is not surprising since both interactions χ_{AS} and χ_{BS} are very small, and there is no driving force for the formation of the inverse structures. A similar result was obtained by Banaszak and Whitmore.¹³ On the other hand, when the solvent is selective for the longer B block ($\chi_{AS} > \chi_{BS} = 0.4$), increasing the solvent selectivity enlarges the C_A microstructure, as shown in Figure 11. Furthermore, we expect that when the copolymer is more asymmetric and/or when more solvent is added, both the C_A and S_A microdomains are broadened due to the effect of solvent selectivity.

To isolate the effect of concentration on the phase behavior, we calculate the two-dimensional phase map for copolymers in terms of ϕ and f when $\chi_{AB}N = 45$, $\chi_{AS} = 0.6$, and $\chi_{BS} = 0.4$ in Figure 12. As expected, when ϕ decreases, the inverse hexagonal cylinders C_A and bcc spheres S_A are observed before the disordered phase is reached for the system $0.5 < f < 0.746$. In general, the effect of solvent concentration on the phase behavior depends on both the selectivity of the solvent and $\chi_{AB}N$. To summarize this effect, we set $\chi_{BS} = 0.4$ and calculated the phase maps of symmetric diblocks as a function of $\chi_{AB}N$, χ_{AS} , and ϕ . Phase transitions similar to those in Figure 9 where $\phi = 0.5$ are obtained for other values of ϕ . Therefore, in Figure 13 we only show the ODT values of $\chi_{AB}N$ between D and S phases as a function of χ_{AS} and ϕ . From Figure 13, the concentration effect on the values of $\chi_{AB}N$ at the ODT (and OOTs) is similar to its effect on the stability limit of a homogeneous phase in Figure 5. Therefore, when the solvent is not very

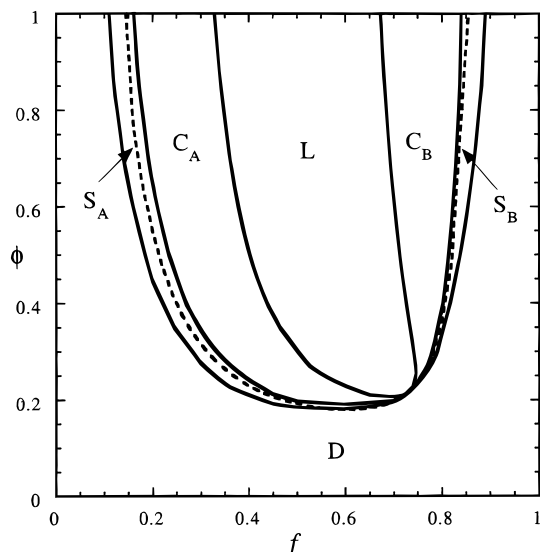


Figure 12. Two-dimensional phase map for a block copolymer solution with $N = 200$, $\chi_{AS} = 0.6$, $\chi_{BS} = 0.4$, and $\chi_{AB}N = 45.0$.

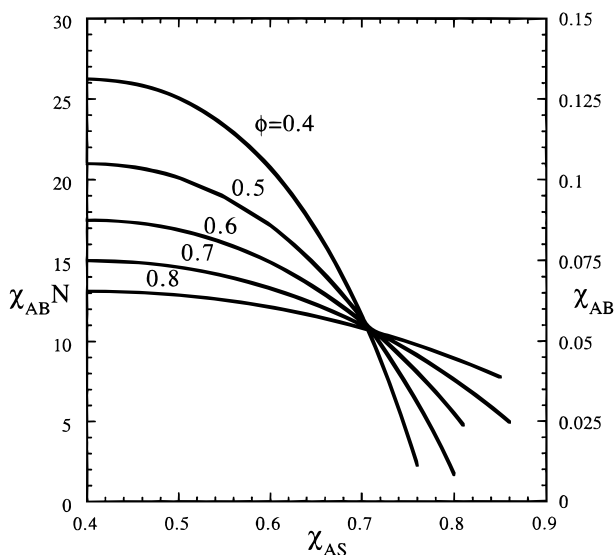


Figure 13. Value of $\chi_{AB}N$ at the ODT as a function of χ_{AS} and ϕ for $f = 0.5$, $N = 200$, and $\chi_{BS} = 0.4$.

selective, e.g., $\chi_{AS} < 0.7$, if we start with a block copolymer melt at a $\chi_{AB}N$ value where the most stable phase is L, as we add more solvent, there should be a sequence of $L \rightarrow C_A \rightarrow S_A \rightarrow D$ transitions. On the other hand, when the solvent selectivity is large, if we start with a disordered symmetric copolymer melt, a sequence of transitions from $D \rightarrow S_A \rightarrow C_A \rightarrow L \rightarrow C_A \rightarrow S_A \rightarrow$ two-phase $D/S \rightarrow D$ is possible.

These predictions can be modified for the effect of solvent amount on the phase behavior of asymmetric block copolymer systems. When the diblock copolymer with $f > 0.5$ is at a constant value of $\chi_{AB}N$, where the melt exhibits the L phase, as more solvent, neutral or selective for A or slightly selective for B, is added, a sequence of $L \rightarrow C_B \rightarrow S_B \rightarrow D$ is expected. It should be noted that the lamellar phase predicted above is eliminated for very asymmetric copolymer systems. In contrast, when the solvent is strongly selective for B, if we start with a disordered melt at a value of $\chi_{AB}N$, as ϕ decreases, the possible phase transition sequence is modified to $D \rightarrow S_B \rightarrow C_B \rightarrow L \rightarrow C_A \rightarrow S_A \rightarrow$ two-phase $D/S \rightarrow D$.

Summary

We have employed self-consistent mean-field (SCMF) theory to examine the phase behavior of block copolymers in the presence of a solvent, focusing on the effects of solvent selectivity and concentration; these results extend the previous studies of Whitmore and co-workers.^{10,13,14} We also applied the RPA method to examine the stability limit of disordered (D) solutions. Phase maps are constructed by comparing free energies of the classical phases: lamellae (L), hexagonal cylinders (C), and bcc spheres (S). Other possible ordered phases, such as the gyroid, are not considered explicitly, and disordered micellar solutions are not examined quantitatively.

In block copolymer melts, the copolymer composition f determines the interfacial curvature, whereas in solutions both solvent selectivity and f strongly influence the morphology. When a neutral solvent is added to a copolymer, the same trends in phase behavior as in melts are expected. The phase maps thus obtained follow the dilution approximation, i.e., by simply replacing $\chi_{AB}N$ in melts with $\phi\chi_{AB}N$. On the other hand, when a slightly selective solvent is added, the dilution approximation fails and different sequences of phase transitions are obtained. For example, in a symmetric copolymer melt or in the presence of a neutral solvent, a transition from $D \rightarrow L$ is expected as $\chi_{AB}N$ increases. In contrast, for the same copolymer in the presence of a selective solvent, e.g., one good for B but poor for A, the progression $D \rightarrow S_A \rightarrow C_A \rightarrow L$ is expected. This transition sequence is also predicted when the solvent is made more selective for B for a fixed value of $\chi_{AB}N$. As the solvent selectivity continues to increase, a further transition from $L \rightarrow C_A \rightarrow S_A \rightarrow$ two-phase occurs. In an asymmetric copolymer system, such as with $f > 0.5$, if the solvent is neutral or selective for A or even slightly selective for B, a sequence of transitions as in melts from $D \rightarrow S_B \rightarrow C_B$ is expected as $\chi_{AB}N$ increases. In general, this solvent selectivity effect enlarges the ordered microstructure regions: as the solvent becomes more selective, the block copolymers tend to form ordered structures at lower $\chi_{AB}N$ values. This trend is consistent with the work of Banaszak and Whitmore on lamellar copolymers in slightly selective solvents.¹³ This effect is very significant when the solvent is strongly selective for the minority B block. In that case, the most stable phase is observed to be L, C_A , or S_A as the selectivity continues to increase. For a constant value of $\chi_{AB}N$, a sequence of transitions due to the effect of increasing solvent selectivity can be summarized as $D \rightarrow S_B \rightarrow C_B \rightarrow L \rightarrow C_A \rightarrow S_A \rightarrow$ two-phase.

The effect of polymer concentration can be summarized as follows. When the solvent is neutral or slightly selective, the $\chi_{AB}N$ values at the ODT and OOT increase as ϕ decreases. Therefore, transitions from $L \rightarrow C \rightarrow S \rightarrow D$ are expected as ϕ decreases. On the other hand, when a strongly selective solvent (for A) is added to a disordered copolymer melt, there can be a sequence of transitions $D \rightarrow S_A \rightarrow C_A \rightarrow L \rightarrow C_B \rightarrow S_B \rightarrow$ (two-phase) $\rightarrow D$. It should be noted that the two-phase macroscopic separation may not occur if the selectivity of the solvent is not large enough. This phenomenon has been observed recently in the PS-PI diblock in the presence of the selective solvent di-*n*-butyl phthalate (DBP).²⁵ The copolymers are asymmetric with $f_{PS} = 0.16$. DBP is good for PS, but it is a Θ solvent for PI near 80 °C. As temperature decreases, DBP becomes

more selective for PS. Therefore, at room temperature, as ϕ decreases from 1.0, the transitions $C_A \rightarrow L \rightarrow C_B \rightarrow S_B \rightarrow$ micelles $\rightarrow D$ were observed. This micellar structure is known to be part of the disordered phase. Since in our calculations the disordered phase is assumed to be homogeneous, this SCMF approach fails to predict this micellar regime. Disordered micelles as well as complex phases will be examined in future work.

Acknowledgment. This work was supported in part by the National Science Foundation, through Grant DMR-9528481 to T.P.L., and by the University of Minnesota Supercomputer Institute, through an allocation of computer time and through a Research Scholarship to C.H. We thank A.-C. Shi, M. W. Matsen, M. D. Whitmore, and F. S. Bates for helpful discussions.

References and Notes

- (1) *Developments in Block Copolymers-1*; Goodman, I., Ed.; Applied Science: New York, 1982.
- (2) *Developments in Block Copolymers-2*; Goodman, I., Ed.; Applied Science: New York, 1985.
- (3) Bates, F. S.; Fredrickson, G. H. *Annu. Rev. Phys. Chem.* **1990**, *41*, 525.
- (4) Fredrickson, G. H.; Bates, F. S. *Annu. Rev. Mater. Sci.* **1996**, *26*, 503.
- (5) Noolandi, J.; Hong, K. M. *Ferroelectrics* **1980**, *30*, 117.
- (6) Hong, K. M.; Noolandi, J. *Macromolecules* **1983**, *16*, 1083.
- (7) Fredrickson, G. H.; Leibler, L. *Macromolecules* **1989**, *22*, 1238.
- (8) Olvera de la Cruz, M. *J. Chem. Phys.* **1989**, *90*, 1995.
- (9) Nagarajan, R.; Ganesh, K. *J. Chem. Phys.* **1989**, *90*, 5843.
- (10) Whitmore, M. D.; Noolandi, J. *J. Chem. Phys.* **1990**, *93*, 2946.
- (11) Halperin, A.; Tirrell, M.; Lodge, T. P. *Adv. Polym. Sci.* **1991**, *100*, 33.
- (12) Yuan, X.-F.; Masters, A. J.; Price, C. *Macromolecules* **1992**, *25*, 6876.
- (13) Banaszak, M.; Whitmore, M. D. *Macromolecules* **1992**, *25*, 3406.
- (14) Whitmore, M. D.; Vavasour, J. D. *Macromolecules* **1992**, *25*, 2041.
- (15) Birshtein, T. M.; Zhulina, E. B. *Polymer* **1990**, *31*, 1312.
- (16) Helfand, E.; Tagami, Y. *J. Chem. Phys.* **1972**, *56*, 3592.
- (17) Shibayama, M.; Hashimoto, T.; Hasegawa, H.; Kawai, H. *Macromolecules* **1983**, *16*, 1427.
- (18) Hashimoto, T.; Shibayama, M.; Kawai, H. *Macromolecules* **1983**, *16*, 1093.
- (19) Lodge, T. P.; Pan, C.; Jin, X.; Liu, Z.; Zhao, J.; Maurer, W. W.; Bates, F. S. *J. Polym. Sci., Polym. Phys. Ed.* **1995**, *33*, 2289.
- (20) Sakurai, S.; Hashimoto, T.; Fetters, L. J. *Macromolecules* **1996**, *29*, 740.
- (21) Mortensen, K.; Pedersen, J. S. *Macromolecules* **1993**, *26*, 805.
- (22) Shibayama, M.; Hashimoto, T.; Kawai, H. *Macromolecules* **1983**, *16*, 16.
- (23) Watanabe, H.; Kotaka, T. *Polym. Eng. Rev.* **1984**, *4*, 73.
- (24) Tuzar, Z.; Kratochvil, P. In *Surface and Colloid Science*; Matijevic, E., Ed.; Plenum Press: New York, 1993; Vol. 15.
- (25) Lodge, T. P.; Xu, X.; Ryu, C. Y.; Hamley, I. W.; Fairclough, J. P. A.; Ryan, A. J.; Pedersen, J. S. *Macromolecules* **1996**, *29*, 5955.
- (26) Lodge, T. P.; Hamersky, M. W.; Hanley, K. J.; Huang, C.-I. *Macromolecules* **1997**, *30*, 6139.
- (27) Matsen, M. W. *Phys. Rev. Lett.* **1995**, *74*, 4225.
- (28) Fredrickson, G. H.; Helfand, E. *J. Chem. Phys.* **1987**, *87*, 697.
- (29) Brazovskii, S. A. *Sov. Phys. JETP* **1975**, *41*, 85.
- (30) Guenza, M.; Schweizer, K. S. *Macromolecules* **1997**, *30*, 4205.
- (31) Matsen, M. W.; Bates, F. S. *Macromolecules* **1996**, *29*, 1091.
- (32) Whitmore, M. D.; Vavasour, J. D. *Acta Polym.* **1995**, *46*, 341.
- (33) *International Tables for X-ray Crystallography*; Henry, N. F. M., Lonsdale, K., Eds.; Kynoch: Birmingham, 1969.
- (34) We employ the term phase map, rather than phase diagram, to emphasize that changing f requires synthesis of a new molecule rather than simple mixing of components.

MA980007P